Electronic Supplementary Material (ESI) for Physical Chemistry Chemical Physics.

Supplementary Information to

The role of the oxime group in the excited state deactivation processes of indirubin

Danîela C. Nobre[a], Estefanía Delgado-Pinar[a,b], Carla Cunha[a], J. Sérgio Seixas de Melo[a]*

[a]University of Coimbra, CQC-ISM, Department of Chemistry, P3004-535 Coimbra, Portugal

[b]Instituto de Ciencia Molecular, Departamento de Química Inorgánica, Universidad de Valencia, C/Catedrático José Beltrán 2, 46980, Paterna, Valencia, Spain

* email: sseixas@ci.uc.pt

Table of Contents

Synthesis of the indirubin derivatives

The synthesis of the indirubin derivatives (see **Scheme SI1**) was achieved by following the general procedure described by Russell and Kaupp[1,2]. Although the synthetic protocol is well-known, some modifications in the work-up and in the purification, step should be added in order to avoid the formation of non-desirable indigo compound[3]. Very briefly, anhydrous methanol was degassed by bubbling nitrogen directly into the solution for 20 min. Then, 3-indoxyl acetate (200 mg, 1.14 mmol), potassium carbonate (1.9 mmol) and the corresponding isatin derivative (1.14 mmol) were added, under stirring, to the round bottom flask keeping the nitrogen bubbling for another 45 min. In all cases, a precipitate is formed, collected by filtration and washed with the appropriate solvent. The purification by column chromatography was performed depending on the derivative.

***N*-methylindirubin (MINR) and indirubin (INR)** were prepared following ref.[3] and ^{1}H, ^{13}C and excitation spectra were used to characterize them and check their purity grade.

6-Bromoindirubin (6-BrINR), (2'Z)-6-Bromoindirubin. 6-bromoisatin was used (258 mg) for the synthesis of (**6-BrINR**). The precipitated obtained was washed with methanol and cold dichloromethane. The filtrate was dried under vacuum and a reddish solid was obtained (323 mg, 83%).

^{1}H NMR (400 MHz, DMSO-d_6) δ (ppm): 8.63 (d, J = 8.3 Hz, 1H, H4), 7.63 (d, J = 7.3 Hz, 1H, H4'), 7.57 (t, J = 7.1 Hz, H6'), 7.39 (d, J = 8.1 Hz, H7'), 7.13 (dd, J = 8.3, 2.0 Hz, H5), 7.03-7.00 (m, H5'-H7). ^{13}C NMR (101 MHz, DMSO-d_6) δ (ppm): 188.6 (C3'), 171.7 (C2), 152.3 (C2'), 144.3 (C7'a), 138.23 (C7a), 136.9 (C6'), 125.6 (C4), 124.2 (C4'), 122.9 (C5), 121.3 (C3a), 121.1 (C5'), 120.9 (C3'a), 118.8 (C6), 113.3 (C7), 112.4 (C7'), 106.1 (C3). ESI-MS (m/z): Calculated for $C_{16}H_9BrN_2O_2$: 341.16; Found $[L + H]^+$: 342.98

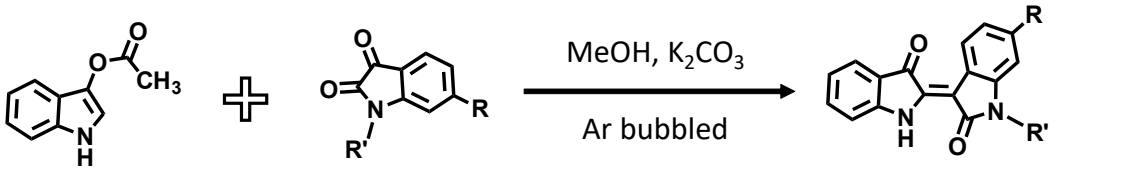

R = H, R' = H; **INR**
R = Br, R' = H; **6-BrINR**
R = H, R' = CH_3; **MINR**

Scheme SI1. Synthetic pathway for the synthesis of **INR**, **6-BrINR** and **MINR**.

Synthesis of the oxime-indirubin derivatives

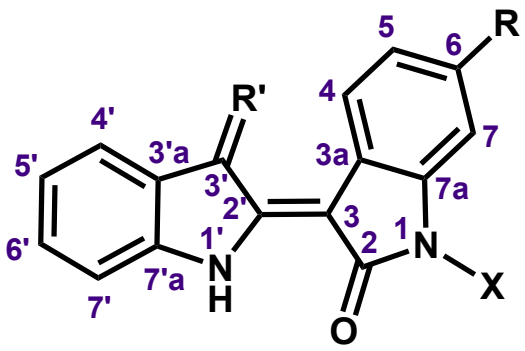

	R	R'	X
INROx	H	N-OH	H
MINROx	H	N-OH	Me
6-Br-INR	Br	O	H
6-Br-INROx	Br	N-OH	H

Scheme SI2. Chemical structures of the indirubin derivatives studied in this work.

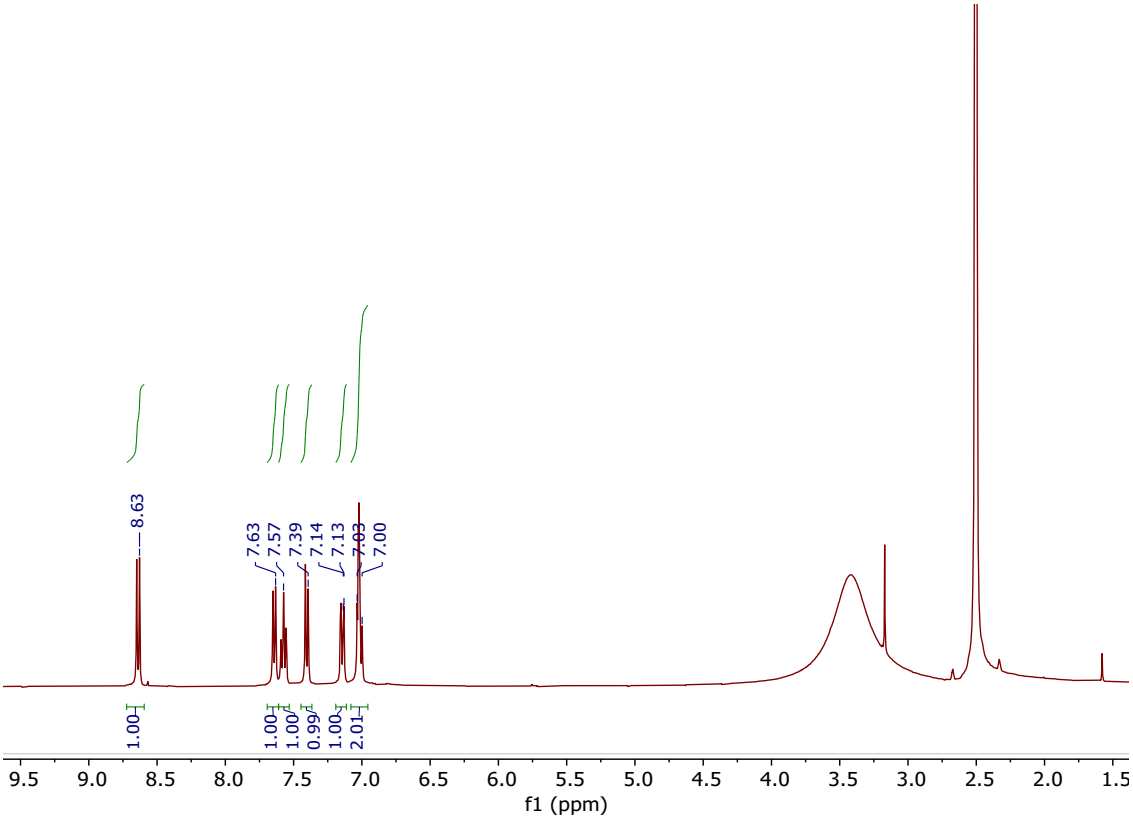

Fig. SI1 ^{1}H NMR spectrum of 6-BrINR in DMSO-d_6.

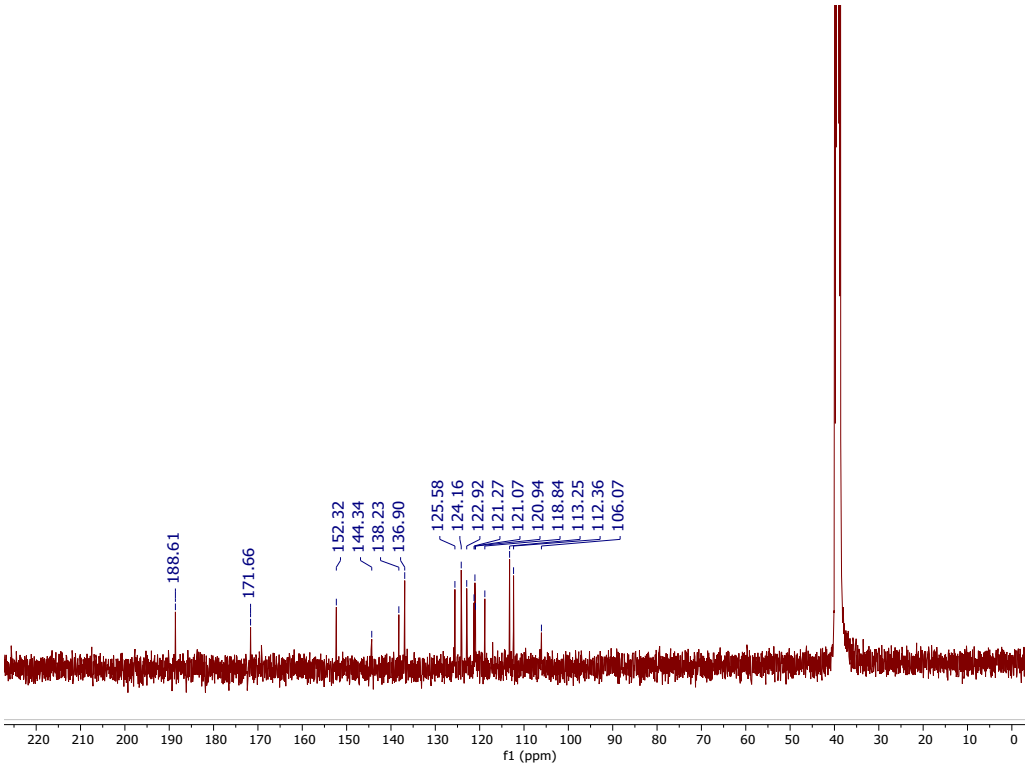

Fig. SI2 ^{13}C NMR spectrum of 6-BrINR in DMSO-d_6.

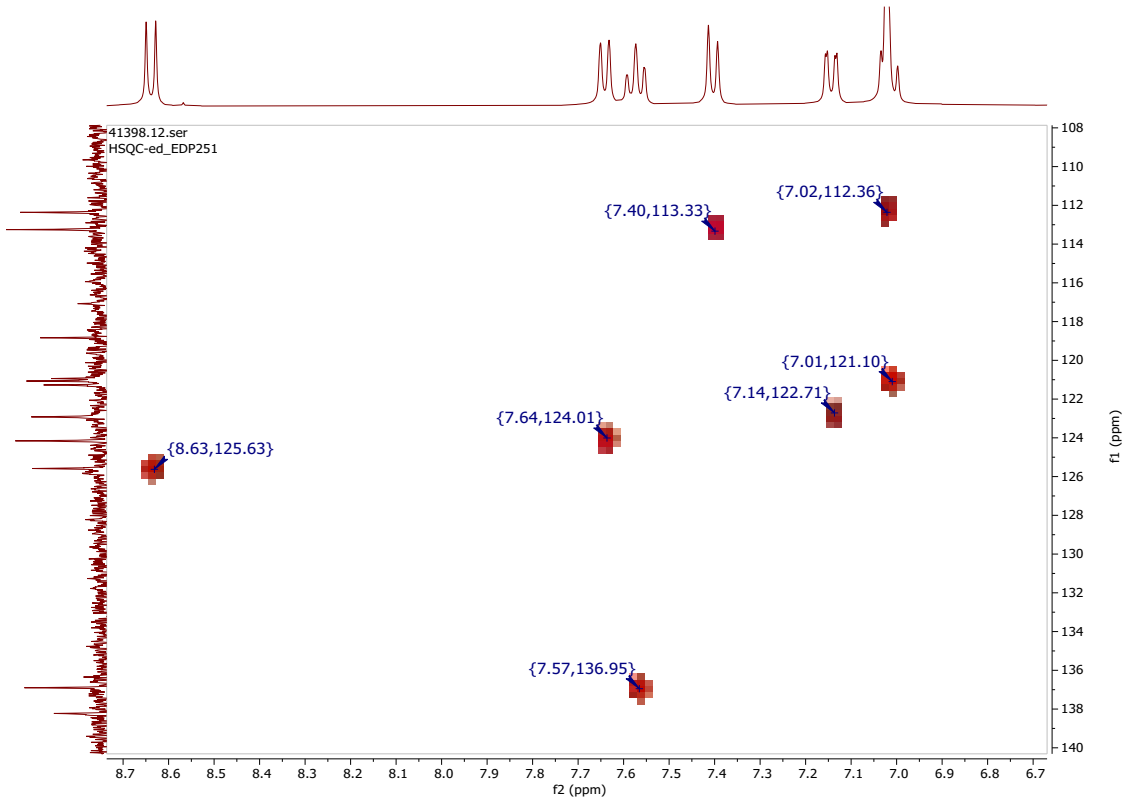

Fig. SI3 HSQC NMR spectrum of 6-BrINR in DMSO-d_6.

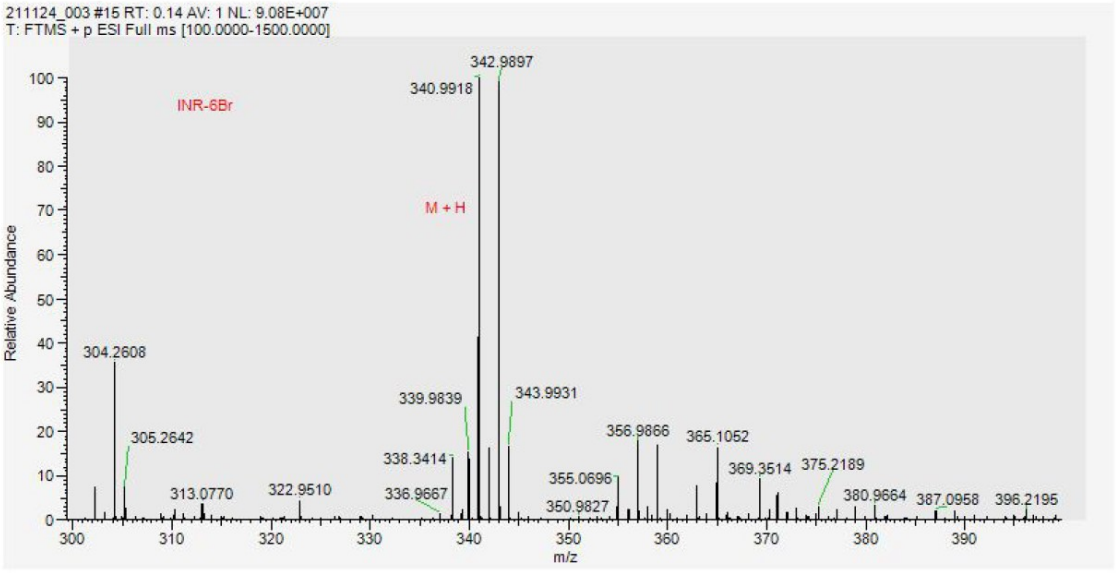

Fig. SI4 Mass spectrum of 6-BrINR.

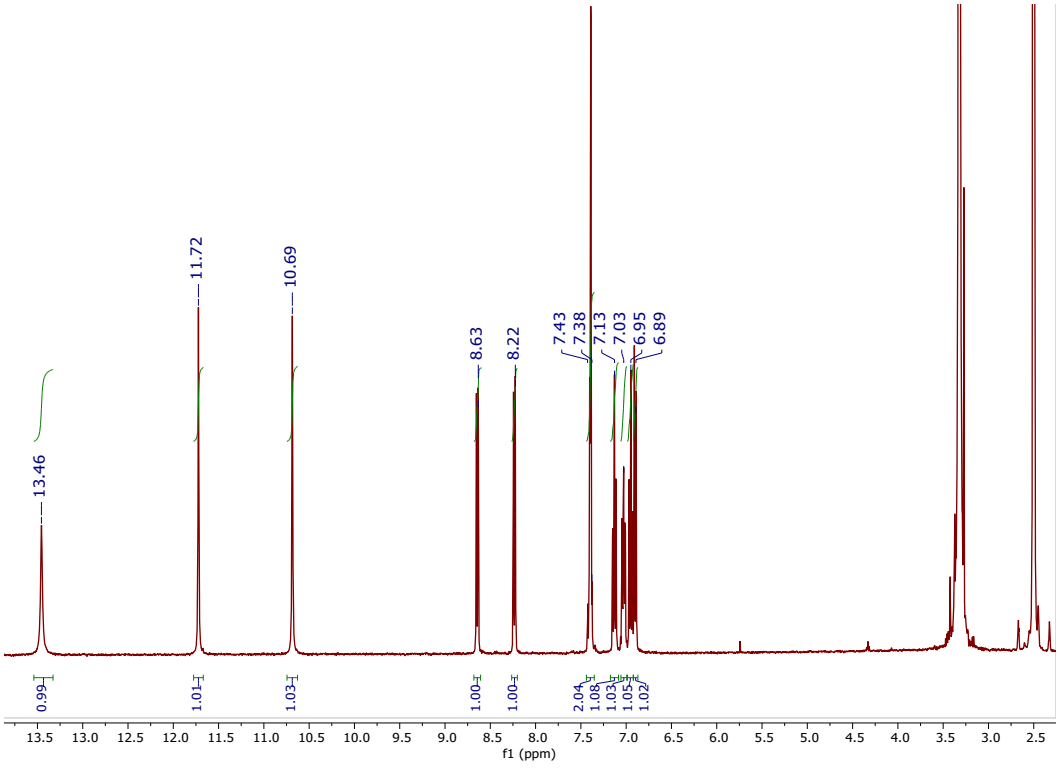

Fig. SI5 ^{1}H NMR spectrum of INROx in DMSO-d_6.

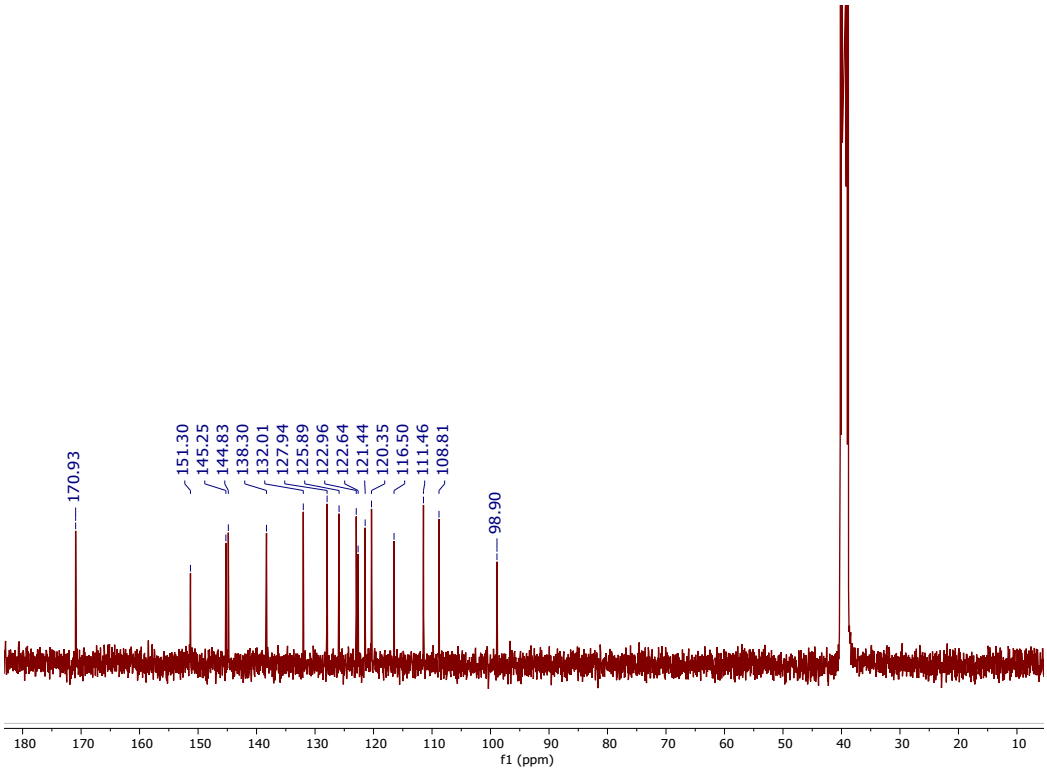

Fig. SI6 ^{13}C NMR spectrum of INROx in DMSO-d_6.

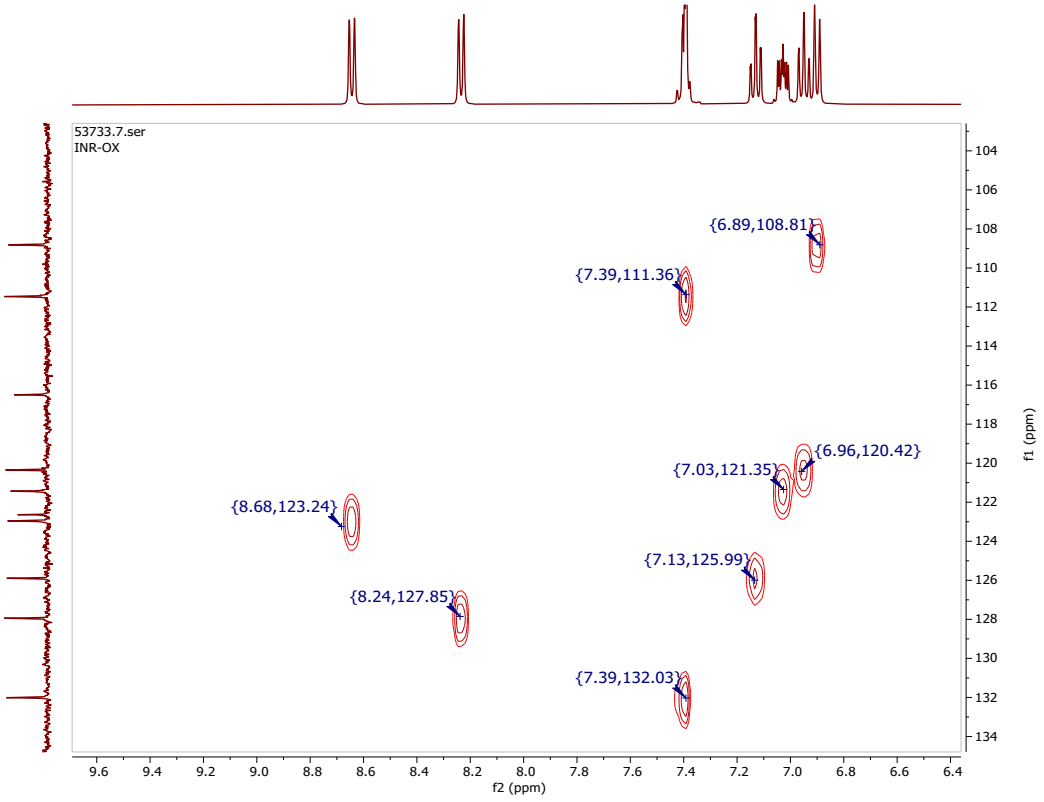

Fig. SI7 HSQC NMR spectrum of INROx in DMSO-d_6.

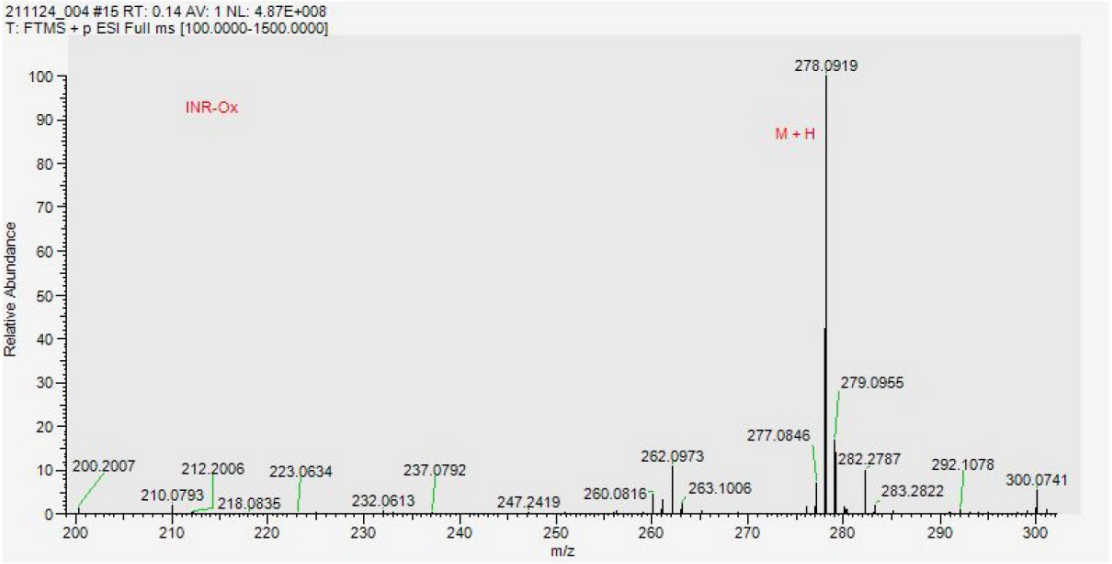

Fig. SI8 Mass spectrum of INROx.

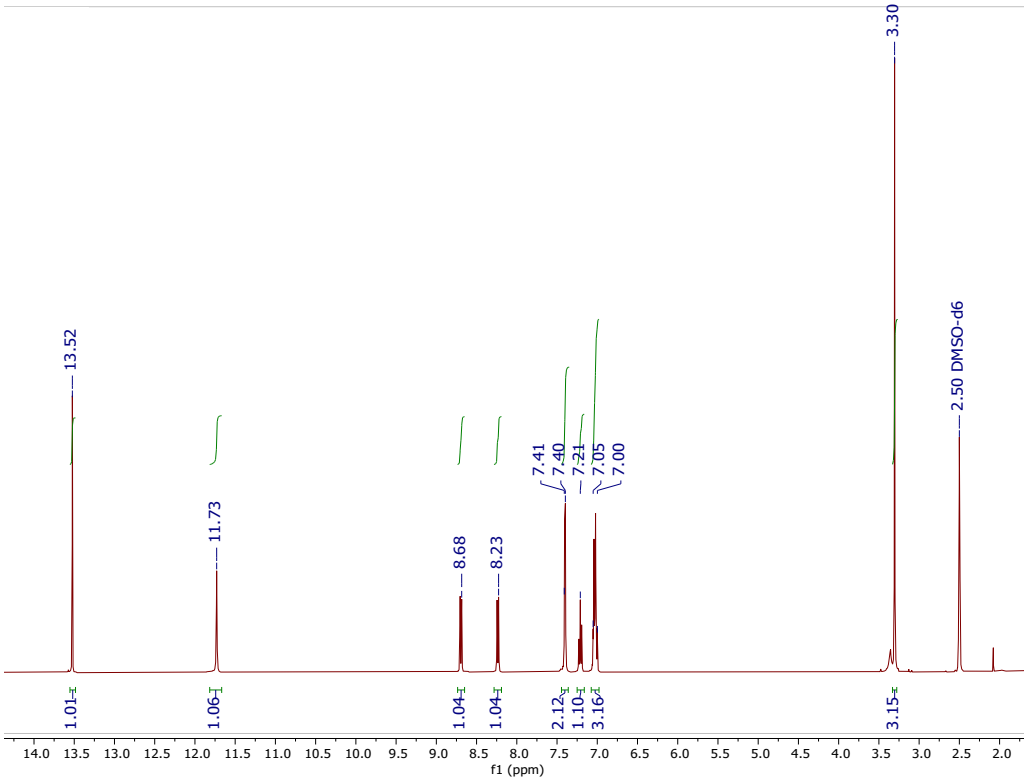

Fig. SI9 ^{1}H NMR spectrum of MINROx in DMSO-d_6.

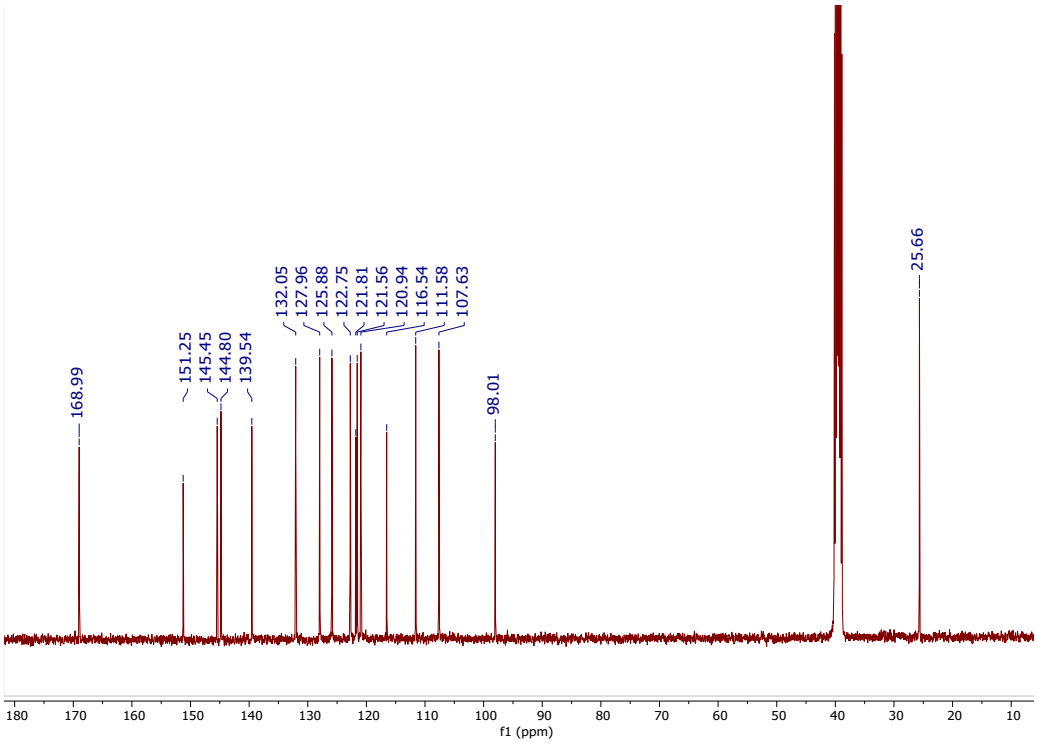

Fig. SI10 ^{13}C NMR spectrum of MINROx in DMSO-d_6.

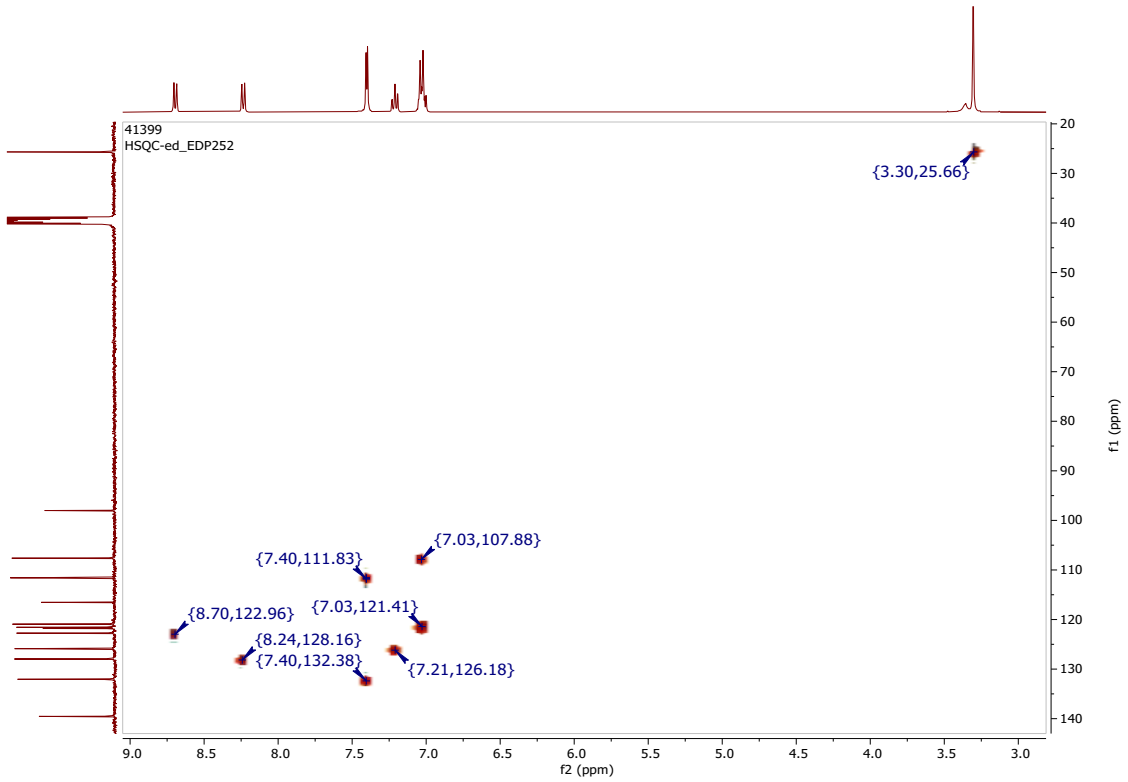

Fig. SI11 HSQC NMR spectrum of MINROx in DMSO-d_6.

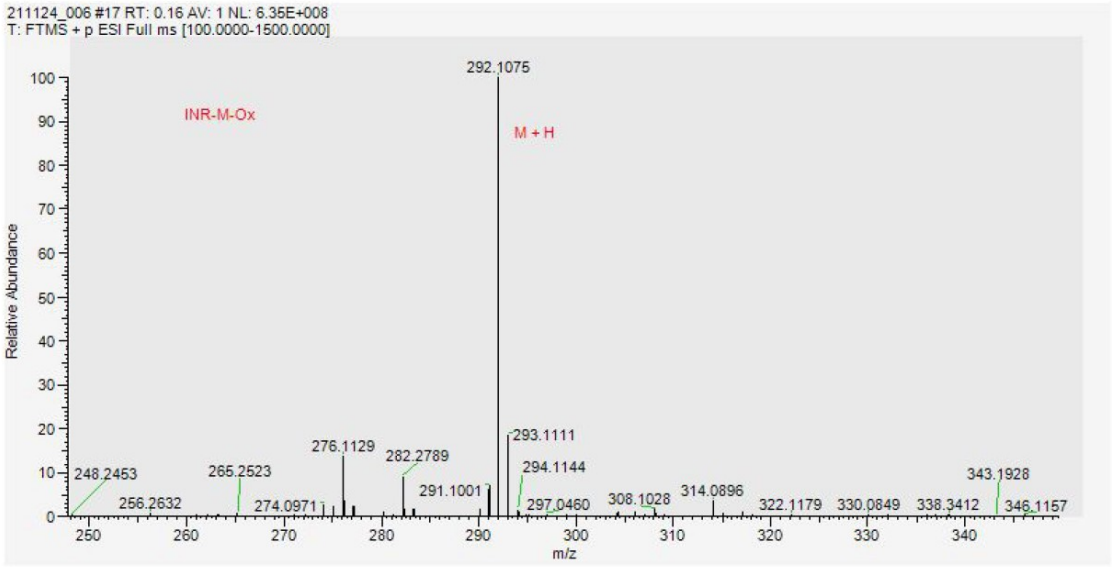

Fig. SI12 Mass spectrum of MINROx.

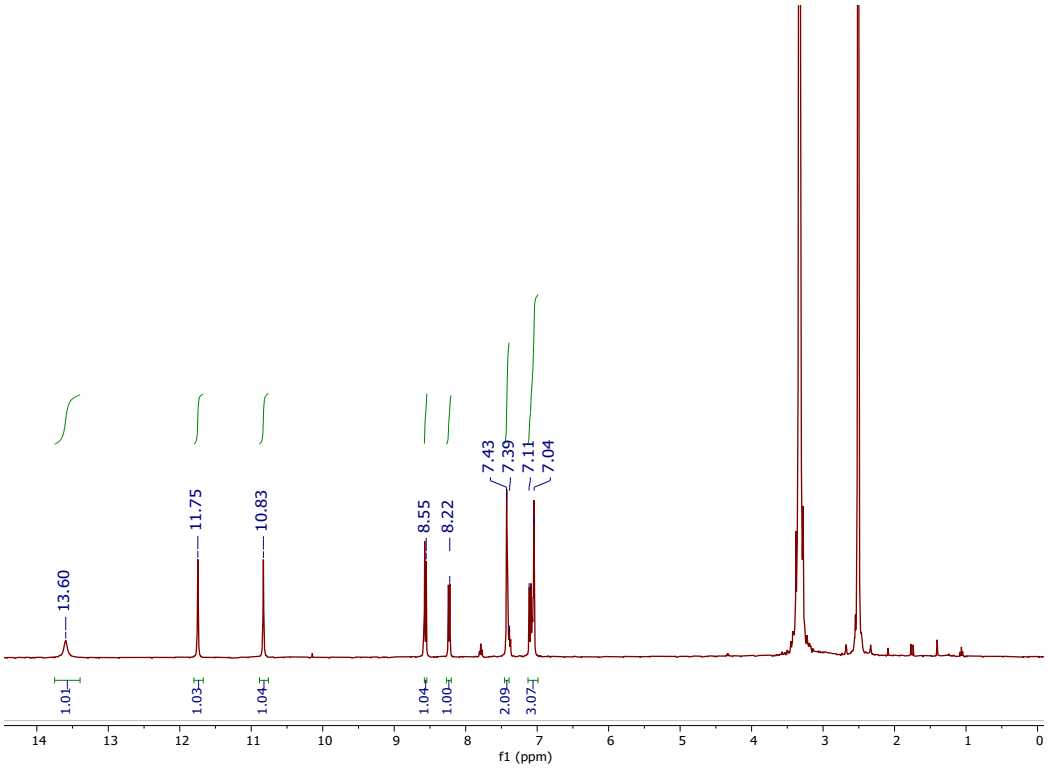

Fig. SI13 ^{1}H NMR spectrum of 6-BrINROx in DMSO-d_6.

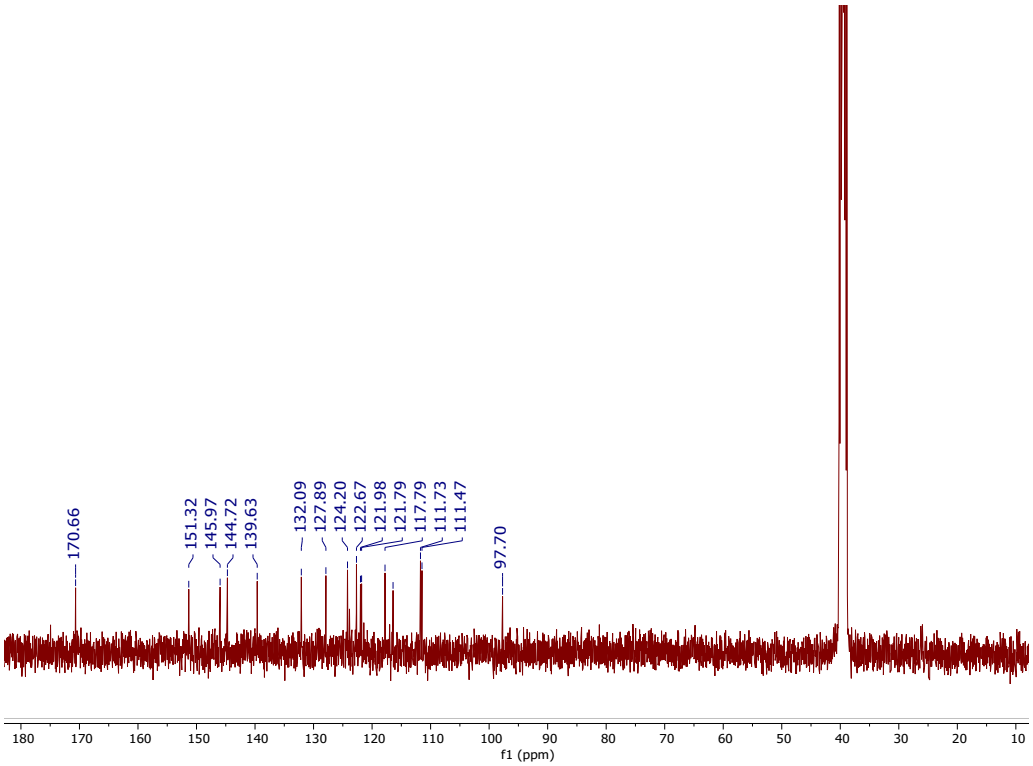

Fig. SI14 ^{13}C NMR spectrum of 6-BrINROx in DMSO-d_6.

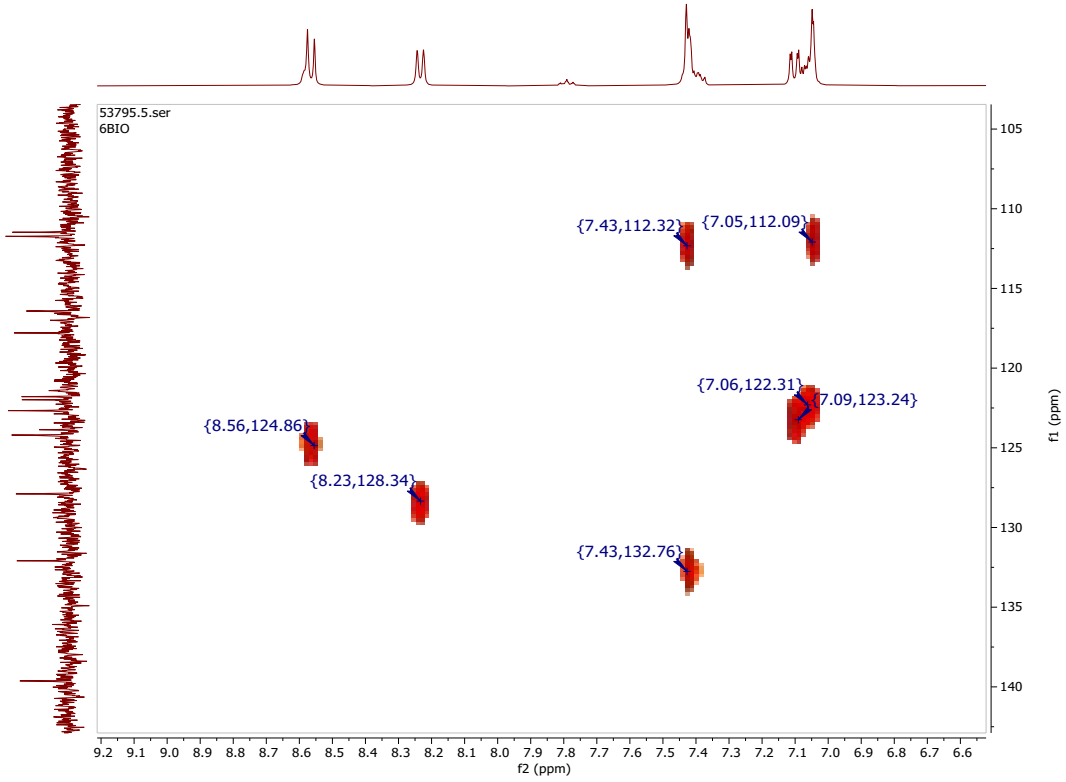

Fig. SI15 HSQC NMR spectrum of 6-BrINROx in DMSO-d_6.

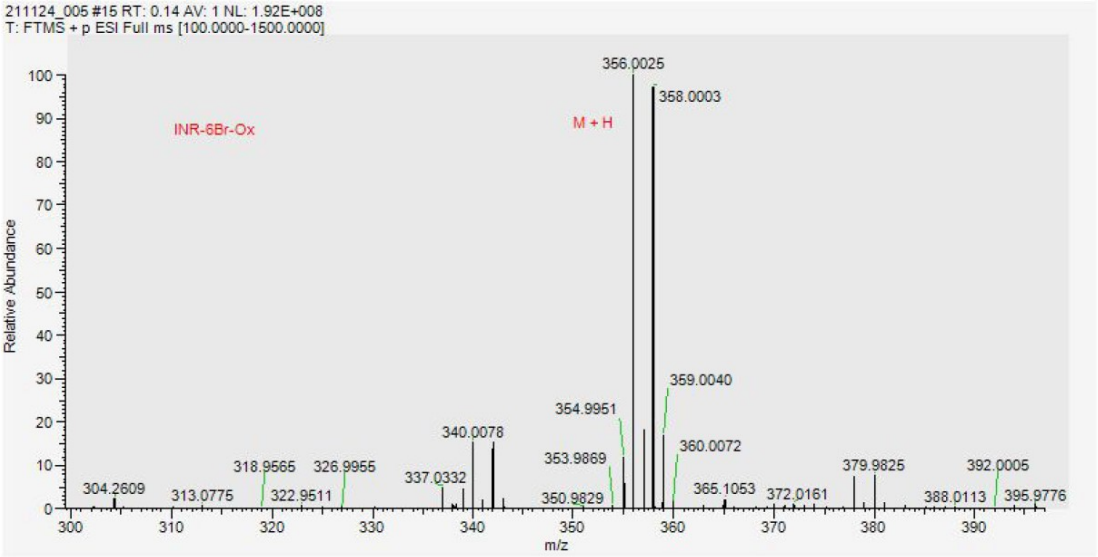

Fig. SI16 Mass spectrum of 6-BrINROx.

Time-Dependent Density Functional Theoretical Calculations

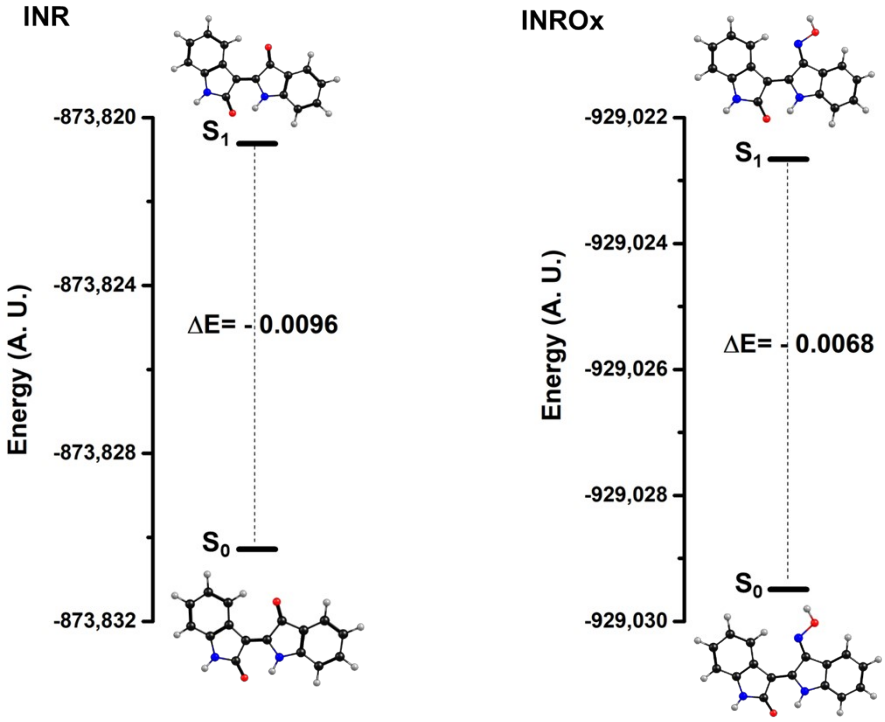

Fig. SI17 Energy difference between the ground state and the first keto singlet excited-state (K-S_1 → K-S_0) for INR and INROx in dioxane.

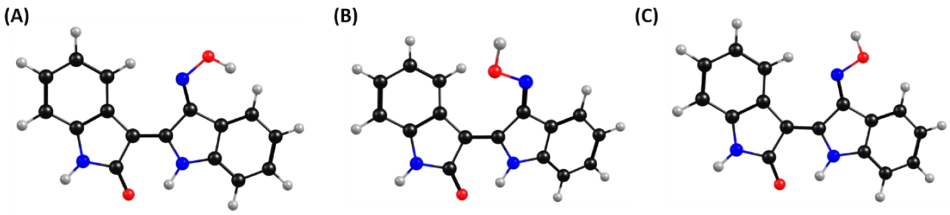

Fig. SI18 Simplified scheme representing the conformational possibilities (structures or conformers A, B, and C) of the oxime-indirubin derivative (INROx).

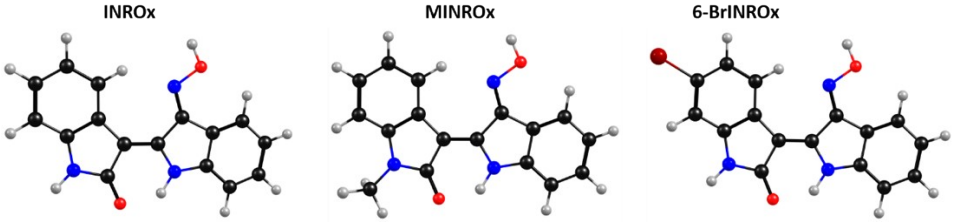

Fig. SI19 Energetically more favourable molecular structures, obtained from TDDFT calculations, for the oxime-indirubin derivatives.

Table SI1. Decay time values, τ_i, obtained from femtosecond Transient Absorption (fs-TA) and femtosecond fluorescence Up Conversion (fs-UC) measurements for INR, INROx, 6-BrINROx, and MINROx, with associated errors, at T=293 K in solvents with varying polarity and viscosity.

Comp.	Solvent	fs-TA		fs-UC	
		τ_1 (ps)	τ_2 (ps)	τ_1 (ps)	τ_2 (ps)
INR[a)]	Dx	-	38	3	37
	MeOH	2	12	-	-
	DMF	1.8	14	1	8
	Glycerol	16	50	-	-
INROx	Dx	0.80±*0.27	6.81±0.12	0.59±0.20	4.03±0.46
	THF	0.74±*0.12	4.99±0.76	0.48±0.20	3.47±0.52
	MeOH	0.72±*0.31	3.71±0.13	-	-
	DMF	0.61±*0.12	3.28±0.78	-	-
	ACN	0.63±*0.24	3.03±0.57	0.58±0.20	2.26±0.18
	Glycerol	4.03±0.26	92.9±0.81	-	-
6-BrINROx	Dx	1.12±*0.28	7.85±0.85	0.9±0.41	4.69±0.44
	THF	0.93±*0.11	5.60±0.59	0.7±0.35	3.29±0.31
	DMF	0.91±*0.24	5.28±0.72	-	-
	ACN	0.42±*0.13	4.13±0.66	0.6±0.20	2.53±0.31
MINROx	Dx	0.80±*0.17	6.79±0.10	0.34±0.23	4.07±0.36
	THF	0.58±*0.36	4.61±0.26	0.5±0.29	4±0.66
	DMF	0.59±*0.14	4.39±0.10	-	-
	ACN	0.50±*0.13	3.50±0.98	0.3±0.20	2.23±0.18

Table SI2. Bond distance between the oxygen in C=O and the hydrogen in N-H for the oxime-indirubin derivatives (INROx, 6-BrINROx and MINROx) obtained using TDDFT calculations in different solvents. The data were obtained at the DFT//LC-BPBE level of theory (ω=0.2).

Compound	Solvent	$d_{C=O\cdots N-H}$ (pm)		$\Delta d_{C=O\cdots N-H}$ (pm)
		S_0	S_1	
INROx	Dx	174.1	162.1	12
	THF	175.2	165.3	9.9
	DMF	174.5	165.0	9.5
	ACN	173.8	164.6	9.2
6-BrINROx	Dx	174.9	164.8	10.1
	THF	175.6	166.5	9.1
	DMF	175.9	168.9	7.0
	ACN	175.5	167.8	7.7
MINROx	Dx	175.2	163.5	11.7
	THF	175.1	166.4	8.7
	DMF	176.9	165.8	11.1
	ACN	176.9	167.2	9.7

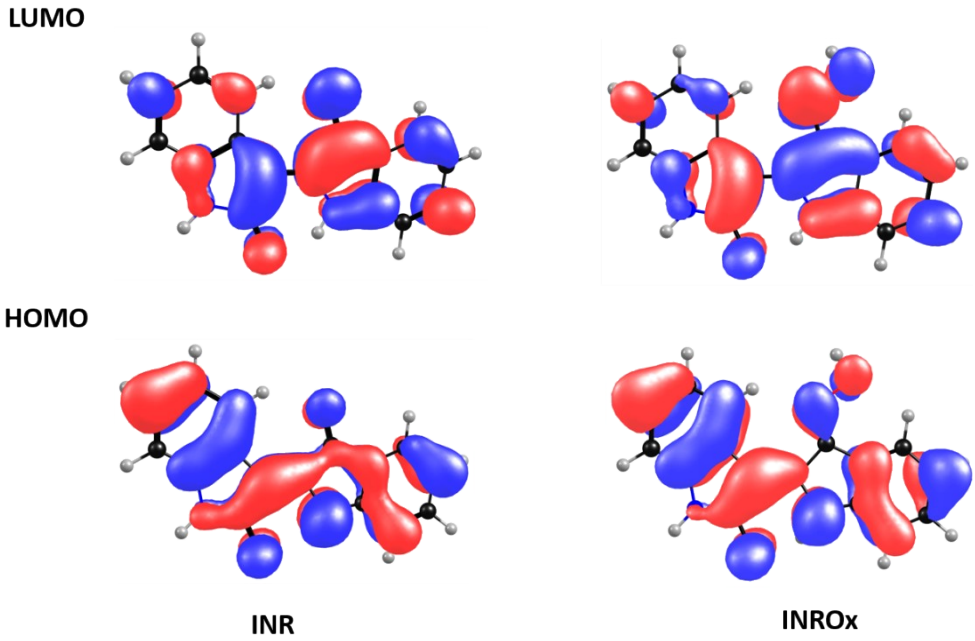

Fig. SI20 Orbital contours of the HOMO and LUMO for indirubin (INR) and oxime-indirubin (INROx) in dioxane.

Table SI3. Wavelength absorption and emission maxima, along with oscillator strengths (*f*), for the keto and enol forms of the indirubin-3'-oxime (INROx) obtained using TDDFT calculations in different solvents. The data were obtained at the DFT//LC-BPBE level of theory (ω=0.2).

Solvent	GS absorption		Species	Emission		TA (transient absorption)		
	nm	*f*		nm	*f*	nm	*f*	S_1 to S_n
Dx	476	0.340	*keto*	545	0.306	569	0.220	$S_1 \rightarrow S_7$
			enol	617	0.199	693	0.248	$S_1 \rightarrow S_3$
						658	0.046	$S_1 \rightarrow S_4$
THF	473	0.339	*keto*	558	0.384	575	0.222	$S_1 \rightarrow S_7$
			enol	618	0.260	700	0.241	$S_1 \rightarrow S_3$
						658	0.044	$S_1 \rightarrow S_4$
DMF	474	0.343	*keto*	566	0.414	576	0.227	$S_1 \rightarrow S_7$
			enol	625	0.287	694	0.242	$S_1 \rightarrow S_3$
						655	0.045	$S_1 \rightarrow S_4$
ACN	471	0.331	*keto*	567	0.415	576	0.224	$S_1 \rightarrow S_7$
			enol	621	0.288	696	0.240	$S_1 \rightarrow S_3$
						658	0.047	$S_1 \rightarrow S_4$

Table SI4. Wavelength absorption and emission maxima, along with oscillator strengths (*f*), for the keto and enol forms of the 6-Bromoindirubin-3'-oxime (6BrINROx) obtained using TDDFT calculations in different solvents. The data were obtained at the DFT//LC-BPBE level of theory (ω=0.2).

Solvent	GS absorption		Species	Emission		TA (transient absorption)		
	nm	*f*		nm	*f*	nm	*f*	S_1 to S_n
Dx	478	0.375	*keto*	546	0.335	567	0.237	$S_1 \rightarrow S_7$
			enol	617	0.212	667	0.050	$S_1 \rightarrow S_3$
						656	0.182	$S_1 \rightarrow S_4$
THF	475	0.374	*keto*	560	0.406	574	0.234	$S_1 \rightarrow S_7$
			enol	617	0.270	669	0.071	$S_1 \rightarrow S_3$
						658	0.157	$S_1 \rightarrow S_4$
DMF	476	0.377	*keto*	564	0.436	577	0.235	$S_1 \rightarrow S_7$
			enol	614	0.306	673	0.110	$S_1 \rightarrow S_3$
						663	0.127	$S_1 \rightarrow S_4$
ACN	473	0.367	*keto*	566	0.436	576	0.234	$S_1 \rightarrow S_7$
			enol	615	0.307	674	0.097	$S_1 \rightarrow S_3$
						665	0.141	$S_1 \rightarrow S_4$

Table SI5. Wavelength absorption and emission maxima, along with oscillator strengths (*f*), for the keto and enol forms of the *N*-methylindirubin-3'-oxime (MINROx) obtained using TDDFT calculations in different solvents. The data were obtained at the DFT//LC-BPBE level of theory (ω=0.2).

Solvent	GS absorption		Species	Emission		TA (transient absorption)		
	nm	*f*		nm	*f*	nm	*f*	S_1 to S_n
Dx	476	0.352	*keto*	543	0.320	570	0.223	$S_1 \rightarrow S_7$
			enol	615	0.213	706	0.304	$S_1 \rightarrow S_3$
						655	0.050	$S_1 \rightarrow S_4$
THF	473	0.351	*keto*	557	0.397	576	0.224	$S_1 \rightarrow S_7$
			enol	617	0.278	710	0.298	$S_1 \rightarrow S_3$
						653	0.052	$S_1 \rightarrow S_4$
DMF	472	0.354	*keto*	565	0.426	576	0.229	$S_1 \rightarrow S_7$
			enol	614	0.312	713	0.299	$S_1 \rightarrow S_3$
						652	0.055	$S_1 \rightarrow S_4$
ACN	470	0.343	*keto*	563	0.429	578	0.226	$S_1 \rightarrow S_7$
			enol	620	0.305	708	0.293	$S_1 \rightarrow S_3$
						655	0.051	$S_1 \rightarrow S_4$

References

1. G. A. Russell and G. Kaupp, *Journal of the American Chemical Society*, 1969, **91**, 3851-3859.
2. R. Hoessel, S. Leclerc, J. A. Endicott, M. E. M. Nobel, A. Lawrie, P. Tunnah, M. Leost, E. Damiens, D. Marie, D. Marko, E. Niederberger, W. Tang, G. Eisenbrand and L. Meijer, *Nature Cell Biology*, 1999, **1**, 60-67.
3. D. C. Nobre, E. Delgado-Pinar, C. Cunha, A. M. Galvão and J. S. Seixas de Melo, *Dyes and Pigments*, 2023, **212**, 111116.